Journal of Nuclear Medicine, published on April 13, 2017 as doi:10.2967/jnumed.116.188789

Cerenkov radiation-induced photoimmunotherapy with ^{18}F-FDG

Yuko Nakamura[1], Tadanobu Nagaya[1], Kazuhide Sato[1], Shuhei Okuyama[1], Fusa Ogata[1], Karen Wong[1], Stephen Adler[1], Peter L. Choyke[1], Hisataka Kobayashi*[1]

[1]Molecular Imaging Program, Center for Cancer Research, National Cancer Institute

*For correspondence or reprints contact: Hisataka Kobayashi, M.D., Ph.D.

Molecular Imaging Program, Center for Cancer Research, National Cancer Institute, NIH, Building 10, RoomB3B69, MSC1088, Bethesda, MD 20892-1088.

Phone: 301-435-4086, Fax: 301-402-3191. E-mail: kobayash@mail.nih.gov

First author: Yuko Nakamura, a fellow of Molecular Imaging Program

Molecular Imaging Program, Center for Cancer Research, National Cancer Institute, NIH, Building 10, RoomB3B69, MSC1088, Bethesda, MD 20892-1088.

Phone: 301-435-4086, Fax: 301-402-3191. E-mail: yuko.nakamura@nih.gov

Word counts: text: 4932, abstract: 176

Financial support

This research was supported by the Intramural Research Program of the National Institute of Health, National Cancer Institute, Center for Cancer Research.

Short running title: Cerenkov radiation-induced PIT

ABSTRACT

Near infrared photoimmunotherapy (NIR-PIT) is a new cancer treatment that combines the specificity of antibodies for targeting tumors with toxicity induced by photo-absorbers after irradiation with NIR light. A limitation of NIR-PIT is the inability to deliver NIR light to a tumor located deep inside the body. Cerenkov radiation (CR) is ultraviolet and blue light which is produced by a charged particle travelling through a dielectric medium faster than the speed of light in that medium and is commonly produced during radioactive decay. Here, we demonstrate the feasibility of using CR generated by ^{18}F-FDG accumulated in tumors to induce photoimmunotherapy.

Methods: Using A431-luc cells therapeutic effects of CR-photoimmunotherapy (CR-PIT) *in vitro* and *in vivo* were evaluated by bioluminescence imaging.

Results: CR-PIT showed significant suppression of tumor size, but the decrease of bioluminescence after CR-PIT was not observed consistently over the entire time course. Conclusion: While CR-PIT can induce tumor killing deep within body, it is less effective than NIR-PIT. This may be related to the relatively lower

efficiency of short wavelength light compared to NIR.

Keywords; photoimmunotherapy, UV-A light, Cerenkov radiation, ^{18}F-FDG

INTRODUCTION

Near infrared photoimmunotherapy (NIR-PIT) is a newly developed cancer treatment that combines the specificity of antibodies for targeting tumors with toxicity induced by photo-absorbers, e.g. IRDye700DX (IR700, silica-phthalocyanine dye), after irradiation with NIR light (*1*). This induces nearly immediate necrotic cell death due to photo-induced cellular membrane damage (*1*,*2*).The first-in-human phase 1 trial of NIR-PIT in patients with inoperable head and neck cancer targeting epidermal growth factor receptor started in June 2015 (https://clinicaltrials.gov/ct2/show/NCT02422979) and has now advanced to a Phase 2 trial in US. Although NIR light can penetrate several centimeters within tissue, an inherent limitation of NIR-PIT is the inability to deliver NIR light directly to a tumor deep within the body (*3*,*4*).

IR700 is a phthalocyanine derivative that typically has a narrow high absorbance in the deep red or near infrared, known as the Q-band and is used for exciting IR700 in NIR-PIT. However, phthalocyanine derivatives, including IR700, have another broad intermediate absorbance peak at around 350 nm (ultra

violet (UV)-A or UV-B)

(https://www.licor.com/bio/products/reagents/irdye/700dx/index.html), also known as the Soret-band, that can be another potential way to excite IR700 (Fig. 1).

Cerenkov radiation (CR) is the ultraviolet and blue light which is produced by a charged particle travelling through a dielectric medium faster than the speed of light in that medium and is commonly produced during radioactive decay (*5*,*6*). CR has been used for 'Cerenkov luminescence imaging', which pairs the production of visible light from radiotracers such as ^{18}F and ^{131}I with widely used small animal optical imaging equipment (*6*-*12*).

The most widely used tracer is the ^{18}F-labeled analog of glucose, 2'-deoxy-2'-[^{18}F]fluoro-D-glucose (^{18}F-FDG), which accumulates in metabolically active cells -such as those in the brain, heart, or a malignant tumor- at a higher rate than other tissues (*13*). CR generated by ionizing radiation has been reported to excite IR700 (*14*). Taken together, tumors located deep in the body could potentially be treated by photoimmunotherapy induced by ^{18}F-FDG

CR.

The purpose of this study was to determine whether CR generated by ^{18}F-FDG could induce photoimmunotherapy in a mouse tumor model.

MATERIALS AND METHODS

Reagents

IRDye 700DX succinimidyl ester was obtained from LI-COR Bioscience (Lincoln, NE, USA). Panitumumab, a fully humanized IgG2 monoclonal antibody (mAb) directed against epidermal growth factor receptor, was purchased from Amgen (Thousand Oaks, CA, USA). Trastuzumab, 95 % humanized IgG_1 mAb directed against human epidermal growth factor receptor type 2 (HER2), was purchased from Genentech (South San Francisco, CA, USA). All other chemicals were of reagent grade.

Synthesis of IR700-conjugated Panitumumab and Trastuzumab

Panitumumab or trastuzumab (1 mg, 6.8 nmol) was incubated with IR700 succinimidyl ester (60.2 μg, 30.8 nmol) in 0.1 mol/L Na_2HPO_4 (pH 8.6) at room temperature for 1 hour. The mixture was purified with a Sephadex G25 column (PD-10; GE Healthcare). The protein concentration was determined with Coomasie Plus protein assay kit (Thermo Fisher Scientific Inc) by measuring the

absorption at 595 nm with spectroscopy (8453 Value System; Agilent Technologies). The concentration of IR700 was measured by the amount of absorbance at 689 nm with spectroscopy to confirm the number of fluorophores conjugated to each mAb. The synthesis was controlled so that an average of two IR700 molecules were bound to a single antibody. We abbreviate IR700 conjugated to panitumumab as pan-IR700, and to trastuzumab as tra-IR700, respectively.

Cell Culture

Epidermal growth factor receptor and luciferase-expressing A431-luc (epidermoid carcinoma of skin/epidermis) and MDAMB468-luc (adenocarcinoma of breast), and HER2 and luciferase-expressing 3T3/HER2-luc cells (fibroblast of embryo) were established. Cell lines were grown in RPMI 1640 (Life Technologies, Gaithersburg, MD, USA) supplemented with 10% fetal bovine serum and 1% penicillin-streptomycin (Life Technologies) in tissue culture flasks in a humidified incubator at 37℃ in an atmosphere of 95 % air and 5 % carbon

dioxide.

In Vitro UV-A-PIT

The majority of CR is in the UV and blue end of the visible spectrum (*6*). Thus, first, we determined the cytotoxic effects of UV-A- photoimmunotherapy (UV-A-PIT) with pan-IR700 for A431-luc and MDAMB468-luc cells or tra-IR700 for 3T3/HER2-luc cells using flow cytometric propidium iodide (Life Technologies, Carlsbad, CA) staining, which can detect compromised cell membranes. Two hundred thousand cells were seeded into 12 well plates and incubated for 24 hours. Medium was replaced with fresh culture medium containing 10 μg/ml of pan-IR700 or tra-IR700 and incubated for 6 hours at 37 ℃. After washing with phosphate buffered saline (PBS), PBS was added and cells were irradiated with a UV-A lamp, which emits light at 365 nm wavelength with 1090 $\mu W/cm^2$ (Spectroline^{TM} E-series handheld lamps, Spectronics Corporation, Westbury, NY, USA). Applied time was 0, 25, 50, 100, 200, 400, 800, and 1600 sec for 0, 0.025, 0.05, 0.1, 0.2, 0.4, 0.8, and 1.6 J/cm^2, respectively. Cells were

scratched 1 hour after treatment. Then PI was added in the cell suspension (final 2 μg/ml) and incubated at room temperature for 30 min, followed by flow cytometry using a flow cytometer (FACS Calibur, BD BioSciences, San Jose, CA, USA) and CellQuest software (BD BioSciences). To evaluate the killing of A431 cells with UV-A light we calculated Δ percentage of surviving cells, based on the ratio of surviving cells exposed to UV-A light with or without pan-IR 700 to those not exposed UV-A light with or without pan-IR700.

In Vitro Cerenkov Radiation-photoimmunotherapy with ^{18}F-FDG

We examined the cytotoxic effects of *in vitro* CR-photoimmunotherapy (CR-PIT) with ^{18}F-FDG by bioluminescence imaging. Five hundred thousand cells were seeded into 12 well plates and incubated for 24 hours. After washing with PBS, 1 ml of phenol red free culture medium was added to each well. 10 μg of pan-IR700 for A431-luc and MDAMB468-luc cells or tra-IR700 for 3T3/HER2-luc cells containing media was added to each well 0.5 hours before adding ^{18}F-FDG. 1 ml of phenol red free culture medium was also added to each

well after washing with PBS before adding ^{18}F-FDG. Shorter incubation time compared to UV-A-PIT was selected because bioluminescence of cancer cells increases rapidly in short time and only 1 hour incubation time with antibody-photo-absorber conjugate (APC) has been reported to induce cytotoxic effect due to NIR-PIT (*1*). For bioluminescence, 150 μg of D-luciferin (Gold Biotechnology, St Louis, MO, USA) was added to each well and analyzed on a bioluminescence imaging system (Photon Imager, Biospace Lab, Paris, France) for luciferase activity -2 (2 hours before), 0 (immediately after), 2, 4, 8 and 24 hours after adding ^{18}F-FDG (the dose of ^{18}F-FDG was 0, 0.11, 0.37, 1.11, 3.7, and 11.1 MBq, respectively). Luciferase activity was reported in relative light units. Regions of interest of similar size were placed on each well encompassing the whole well and the sum of relative light units was calculated using M^3 Vision Software (Biospace Lab). Next, the luciferase activity ratio was calculated from each value divided by baseline value.

Animal Model

We performed an animal study only using the A431-luc tumor model because clear CR-PIT effect was confirmed *in vitro* using this cell line. All procedures were performed in compliance with the Guide for the Care and Use of Laboratory Animals (*15*) and approved by NCI-Bethesda Animal Care and Use Committee. Six- to 8-week old female homozygote athymic nude mice were purchased from Charles River (National Cancer Institute, Frederick, MD). A431-luc cells (2×10^6 in PBS) were injected subcutaneously in the right dorsum of the mice under isoflurane anesthesia. Experiments were conducted at 5 days after cell injection.

In Vivo Cerenkov Radiation-photoimmunotherapy with ^{18}F-FDG

Tumor bearing mice were randomized into 4 groups at least 10 animals per group for the following treatments: (1) no treatment (control); (2) 200 μg of pan-IR700 i.v. (APC i.v. only); (3) 37 MBq of ^{18}F-FDG injection only (^{18}F-FDG only); (4) 200 μg of pan-IR700 i.v., and 37 MBq of ^{18}F-FDG was administered on day 1 after injection of APC (CR-PIT). This ^{18}F-FDG dose was selected because

37 MBq was the maximum dose that can be given to a mouse without inducing cytotoxic effects in the A431-luc tumor cells (data not shown).

Under anesthesia, tumor-bearing mice were administered 37 MBq of ^{18}F-FDG intravenously. All injections of ^{18}F-FDG were performed in the late morning with fasting from the evening before as that can affect the ^{18}F-FDG biodistribution (*16*). At 5 hours after ^{18}F-FDG injection, the mice were imaged under anesthesia with 2-3 % isoflurane using BioPET/CT (Bioscan Inc., Washington, DC, USA) to confirm biologic uptake. This time was selected to allow sufficient decay because the maximum dose of ^{18}F-FDG that still provides accurate measurement on this scanner is around 11.1 MBq. Both PET and CT imaging data were acquired. The PET images were acquired using an energy window of 250-700 keV. The PET images were reconstructed using a Fourier re-binning algorithm to generate 2D sinograms from the 3D list mode data. The sinograms were corrected for randoms, scatter, and detector normalization artefacts. CT based attenuation correction was also applied to the sinograms. The fully corrected sinograms were reconstructed into images using an ordered-subset

expectation maximization algorithm. CT images of the mice were acquired using an X-ray tube voltage and current settings of 50 kV and 180 mA respectively and reconstructed using a filtered back projection algorithm.

The treatment effects were determined with relative bioluminescence measured before and after treatment. For bioluminescence, D-luciferin (15 mg/ml, 200 µl) was injected intraperitoneally and the mice were analyzed with a Photon Imager for luciferase activity before, 8, and 24 hours after ^{18}F-FDG injection. Regions of interests of similar size were placed over each tumor.

Hepatotoxicity Induced by Cerenkov Radiation-photoimmunotherapy with ^{18}F-FDG

Hepatotoxicity may result from CR-PIT due to accumulating both ^{18}F-FDG and APC in liver. To validate the degree of hepatotoxicity due to CR-PIT mice were randomized into 4 groups with at least 2 animals per group for the following treatments: (1) no treatment (control); (2) 300 µg of pan-IR700 i.v. (APC i.v. only); (3) 300 µg of pan-IR700 i.v. and then 40 J/cm^2 of NIR light

exposed to the liver at on day 1 after injection of APC (NIR-PIT); (4) 300 μg of pan-IR700 i.v., and 111 MBq of ^{18}F-FDG was administered on day 1 after injection of APC (CR-PIT). NIR light was exposed to the liver using NIR laser light at 685 to 693 nm wavelength (BWF5-690-8-500-0.37; B&W TEK INC., Newark, DE, USA) while the remainder of the body was shielded from light with aluminum foil.

Pathological Analysis for Treated Tumor and the Liver

To evaluate histological changes after CR-PIT, light microscopy was performed using an Olympus BX61 microscope (Olympus America, Inc., Melville, NY). A431-luc tumors were excised from control mice, 24 hours after injection of pan-IR700 (APC i.v. only), 24 hours after injection of ^{18}F-FDG (^{18}F-FDG only), and 24 hours after CR-PIT. Livers were also removed from control mice, 24 hours after injection of pan-IR700 (APC i.v. only), 24 hours after NIR-PIT, and 24 hours after CR-PIT. Tumors and livers were placed in 10 % formalin and serial 10 μm slice sections were fixed on glass slides with hematoxylin and eosin staining.

Statistical Analysis

Statistical analysis was performed with JMP 10 software (SAS Institute, Cary, NC). Data are expressed as means ± s.e.m. from a minimum of four experiments, unless otherwise indicated. We determined the differences in each percentage of surviving cells compared to the value without UV-A light or APC (control) using Dunnett's correction for multiple comparison. For evaluation of luciferase activity we also determined each luciferase activity ratio compared to the value at starting point for *in vitro* and controls (group 1) *in vivo* using Dunnett's correction for multiple comparison. Differences of $p < 0.05$ were considered statistically significant.

RESULTS

In Vitro UV-A-PIT

A431-luc cells. Percentage of surviving cells decreased in a light dose dependent manner ($p < 0.01$ for 0.025, 0.05, 0.1, 0.2, 0.4, 0.8, and 1.6 J of UV-A light with pan-IR700 compared to the value without UV-A light or pan-IR700) (Fig. 2A). However, significant cytotoxicity associated with UV-A light alone (over 0.8 J) was seen in the absence of pan-IR700 and with pan-IR700 alone but no UV-A light (Fig. 2A). Δ percentage of surviving cells increased in a light dose dependent manner with pan-IR700 while Δ percentage of surviving cells was negligible up to 0.4 J of UV-A light irradiation without pan-IR700. Thus, we concluded that UV-A light with pan-IR700 induce cell death because of the photoimmunotherapy effect (Supplemental Fig. 1).

MDAMB468-luc cells. Percentage of surviving cells decreased in a light dose dependent manner ($p = 0.11$ for 0.025 J, $p < 0.01$ for 0.05, 0.1, 0.2, 0.4, 0.8, and 1.6 J of UV-A light with pan-IR700 compared to the value without UV-A

light or pan-IR700) (Fig. 2B). However, significant cytotoxicity associated with UV-A light alone in the absence of pan-IR700 was observed ($p < 0.01$ for 0.1, 0.2, 0.4, 0.8, and 1.6 J compared to the value without UV-A light or pan-IR700) (Fig. 2B).

3T3/HER2-luc cells. Percentage of surviving cells decreased in a light dose dependent manner ($p = 0.04$ for 0.025 J, $p < 0.01$ for 0.05, 0.1, 0.2, 0.4, 0.8, and 1.6 J of UV-A light with tra-IR700 compared to the value without UV-A light or tra-IR700) (Fig. 2C). There was no significant cytotoxicity associated with UV-A light alone in the absence of tra-IR700 compared to without UV-A light or tra-IR700.

In Vitro Cerenkov Radiation-photoimmunotherapy with ^{18}F-FDG

A431-luc cells. There was no significant difference in luciferase activity ratio between 0 and -2 hour with pan-IR700 and ^{18}F-FDG ($p = 0.09$, 0.42, 0.38, 0.27, and 0.64 for 0.11, 0.37, 1.11, 3.7, and 11.1 MBq of ^{18}F-FDG administration,

respectively) (Fig. 3A). Luciferase activity ratio increased significantly at 2, 8, and 24 hours after ^{18}F-FDG administration compared to that at -2 hour with and without ^{18}F-FDG ($p < 0.01$ for all). On the other hand, without pan-IR700 luciferase activity ratio increased significantly at all time points including 0 hour compared to that at -2 hour regardless of presence or absence of ^{18}F-FDG ($p < 0.01$ for all) (Fig. 3A). Taken together, CR-PIT from ^{18}F-FDG had a demonstrable effect on A431-luc cells *in vitro*.

MDAMB468-luc cells. In the absence of pan-IR700, luciferase activity ratio increased significantly at 0 hour compared to that at -2 hour up to 1.11 MBq of ^{18}F-FDG administration ($p < 0.01$ for 0, 0.11, 0.37, and 1.11 MBq of ^{18}F-FDG administration, respectively), while there was no significant difference in luciferase activity ratio between 0 and -2 hour when the dose was increased to 3.7 or 11.1 MBq of ^{18}F-FDG ($p = 0.37$ and 0.97 for 3.7 and 11.1 MBq of ^{18}F-FDG administration, respectively) (Fig. 3B). Moreover, when pan-IR700 was given, luciferase activity ratio increased significantly at all time points including 0 hour

compared to that at -2 hour with and without ^{18}F-FDG ($p < 0.01$ for all) (Fig. 3B). These results suggested that the effect of CR-PIT could not be observed *in vitro* using MDAMB468-luc cells.

3T3/HER2-luc cells. In the absence of tra-IR700, luciferase activity ratio increased significantly at 0 hour compared to that at -2 hour up to 0.37 MBq of ^{18}F-FDG administration ($p < 0.01$ for 0, 0.11, and 0.37 MBq of ^{18}F-FDG administration, respectively), while there was no significant difference in luciferase activity when more than 1.11 MBq of ^{18}F-FDG was administered ($p = 0.05$, 0.58, and 0.78 for 1.11, 3.7, and 11.1 MBq of ^{18}F-FDG administration, respectively) (Fig. 3C), suggesting that cytotoxicity might be induced by CR derived from ^{18}F-FDG *in vitro*. In the presence of tra-IR700, luciferase activity increased significantly with administration of 11.1 MBq of ^{18}F-FDG ($p = 0.03$), although there was no significant difference in luciferase activity ratio between 0 and -2 hour with administration of ^{18}F-FDG up to 3.7 MBq ($p = 0.71$, 0.24, and 0.20 for 0.11, 0.37, 1.11, and 3.7 MBq of ^{18}F-FDG administration, respectively)

(Fig. 3C). Thus, the effect of CR-PIT was unpredictable *in vitro* using 3T3/HER2 cells.

In Vivo Cerenkov Radiation-photoimmunotherapy with ^{18}F-FDG

The treatment regimen is shown in Fig. 4A. ^{18}F-FDG clearly accumulated within the tumor (Fig. 4B). In the control, APC i.v. only, and ^{18}F-FDG only group luciferase activity of tumors increased rapidly with time indicating tumor growth. On the other hand, in the CR-PIT group luciferase activity of tumors increased at a lower rate (Figs. 4C and 5A). 8 hours after ^{18}F-FDG injection the post/pre ^{18}F-FDG luciferase activity ratio in the CR-PIT group was significantly lower compared to that in the control group, while there was no significant difference in luciferase activity in APC i.v. only and ^{18}F-FDG only group compared to the control ($p = 0.83$, 0.54, and 0.04 for APC i.v. only, ^{18}F-FDG only, and CR-PIT group, respectively) (Fig. 5B). 24 hours after ^{18}F-FDG injection post/pre ^{18}F-FDG luciferase activity ratio in the CR-PIT group was also significantly lower compared to that in controls ($p = 0.05$). However, there was no significant

difference in luciferase activity in APC i.v. only and ^{18}F-FDG only group compared to controls ($p = 0.47$ and 0.85 for APC i.v. only and ^{18}F-FDG only, respectively) (Fig. 5B).

Pathological Analysis for Treated Tumor and the Liver

CR-PIT treated tumors showed cellular necrosis and micro-hemorrhage within a background of live but damaged tumor cells while little damage was observed in tumors receiving ^{18}F-FDG only (Fig. 6). This appearance is similar but milder to that observed with conventional NIR-PIT. No obvious damage was observed in tumors in the APC i.v. only and control groups (Fig. 6).

The livers treated with NIR-PIT showed yellowish color changes on the surface in macroscopic appearance and extensive hepatic cell damage especially at the peri-Glisson's capsule area on microscopic images (Supplemental Fig. 2). On the other hand, the livers treated with CR-PIT showed mild hepatic cell damage mainly at the peri-Glisson's capsule area on microscopic images, however, there was no obvious change in macroscopic surface appearance. No obvious

damage was observed in the livers in the APC *i.v.* only and control groups (Supplemental Fig. 2).

DISCUSSION

From our result we found that UV-A light can induce photoimmunotherapy. However, some cells are quite sensitive to the effects of UV-A light alone as shown in MDAMB468-luc cells, suggesting that some cancer cells (as well as normal cells) are highly sensitive to UV-A light by itself whereas NIR light is completely harmless by itself (*1*,*17*,*18*).

The *in vitro* results of CR-PIT suggested that among the cells tested, A431-luc cells were more sensitive than MDAMB468-luc and 3T3/HER2 cells. This may be because CR and radiation exposure itself may induce variable cytotoxicity in certain cell lines (*19*), resulting in reduced additional cytotoxic effects of CR-PIT. Variability in this effect may be traced to variable accumulation of ^{18}F-FDG in each cell type (*20*). Alternatively, the light produced by CR may be insufficient to induce photoimmunotherapy effects in these cell lines.

CR-PIT for A431-luc tumor showed significant inhibition of luciferase activity *in vivo*. Moreover, pathological analysis revealed cellular necrosis and micro-hemorrhage within the CR-PIT treated tumor, indicating that CR-PIT was

capable of inhibiting A431-luc tumor growth.

The decrease of luciferase activity after CR-PIT in A431-luc tumors was not observed consistently over the entire time course of the experiment unlike NIR-PIT (*1*). This suggests CR-PIT was less effective than NIR-PIT. First, photoimmunotherapy depends on light absorption by the photo-absorber, IR700, which is optimally excited at 689 nm. UV-A light at 350 nm is only 1/3 as effective as NIR. Furthermore, compared to NIR, CR is much lower in intensity and penetrates only 1-2 mm into tissue. Moreover, CR is emitted inside of the cell and lipid cell membrane has the capacity to absorb UV light including CR (*13,20*). Therefore, only a small part of CR may reach IR700 on the cell membrane (*1*).

One approach would be to inject a larger dose of ^{18}F-FDG with proportionately more CR. However, one is limited by the permissible radiation dose in humans. Moreover, hepatotoxicity could result from CR-PIT in the liver due to accumulation of both ^{18}F-FDG and APC. Mild hepatic cell damage was observed in peri-Glisson's capsule area, however, this damage was diffuse throughout the liver suggesting potential for significant hepatotoxicity. Therefore,

in the future, it might be preferable to select PET agents and Ab-IR700 conjugates that demonstrate less hepatic uptake than ^{18}F-FDG or pan-IR700.

Selecting an alternative radionuclide that emits high energy beta-radiation with high yield CR is a potential way to improve the effect of CR-PIT (*6,12,21,22*). However, the labeled agent must be highly tropic to cancer with little off-target accumulation and the half-life and dosimetry must be such that acceptable exposure to non-target organs can be achieved while still producing enough light for CR-PIT.

CR-activated photosensitizer-labeled nanoparticles have been reported (*8,23,24*). However, unlike NIR-PIT, none of photosensitizer labeled nanoparticles has been used in clinical trials. Another concern with CR-activated photosensitizer-labeled nanoparticles is inferior selectivity because the CR emitted from these nanoparticles cannot be directed exclusively to the tumor area (*1*). In contrast NIR-PIT is highly selective for tumor. Thus, we think CR-PIT may be a better approach compared to CR-activated photosensitizer labeled nanoparticles.

Since CR-PIT has less immediate efficacy compared to NIR-PIT we did not conduct a long term evaluation because tumors re-grew quickly, resulting in no significant therapeutic effect. However, CR clearly induced cytotoxic photoimmunotherapy *in vivo*, indicating that, similar to NIR-PIT, CR-PIT has the potential to activate anti-cancer host immunity by inducing immunogenic cell death either by CR-PIT or by employing an antibody-conjugate that selectively targets tumor-associated regulatory T cells (*2*,*25*).

CONCLUSION

CR-PIT using ^{18}F-FDG showed significant therapeutic effects when using A431-luc cells *in vitro* and *in vivo*. Although, CR-PIT is less effective than NIR-PIT, it could nevertheless have an impact for treating tumors located deep within the body where NIR light cannot reach. Specific developments that might aid the effectiveness of CR-PIT include the development of specific radioactive probes that emit more CR but have lower hepatic accumulation.

ACKNOWLEDGEMENT

The authors thank Anita Ton Thien for reconstruction of PET images and Philip C.

Eclarinal for management of ^{18}F-FDG.

REFERENCES

1. Mitsunaga M, Ogawa M, Kosaka N, Rosenblum LT, Choyke PL, Kobayashi H. Cancer cell-selective in vivo near infrared photoimmunotherapy targeting specific membrane molecules. *Nat Med.* 2011;17:1685-1691.

2. Ogawa M, Tomita Y, Nakamura Y, et al. Immunogenic cancer cell death selectively induced by near infrared photoimmunotherapy initiates host tumor immunity. *Oncotarget.* 2017;8:10425-10436.

3. Ai X, Mu J, Xing B. Recent advances of light-mediated theranostics. *Theranostics.* 2016;6:2439-2457.

4. Hudson DE, Hudson DO, Wininger JM, Richardson BD. Penetration of laser light at 808 and 980 nm in bovine tissue samples. *Photomed Laser Surg.* 2013;31:163-168.

5. Cerenkov PA. Visible emission of clean liquids by action of γ radiation. *C R Dokl Akad Nauk SSSR.* 1934;2:451-454.

6. Thorek D, Robertson R, Bacchus WA, et al. Cerenkov imaging - a new modality for molecular imaging. *Am J Nucl Med Mol Imaging.* 2012;2:163-173.

7. Robertson R, Germanos MS, Li C, Mitchell GS, Cherry SR, Silva MD. Optical imaging of Cerenkov light generation from positron-emitting radiotracers. *Phys Med Biol.* 2009;54:N355-365.

8. Shaffer TM, Drain CM, Grimm J. Optical imaging of ionizing radiation from clinical sources. *J Nucl Med.* 2016;57:1661-1666.

9. Thorek DL, Riedl CC, Grimm J. Clinical Cerenkov luminescence imaging of (18)F-FDG. *J Nucl Med.* 2014;55:95-98.

10. Zhang X, Kuo C, Moore A, Ran C. In vivo optical imaging of interscapular brown adipose tissue with (18)F-FDG via Cerenkov luminescence imaging. *PLoS One.* 2013;8:e62007.

11. Spinelli AE, D'Ambrosio D, Calderan L, Marengo M, Sbarbati A, Boschi F. Cerenkov radiation allows in vivo optical imaging of positron emitting radiotracers. *Phys Med Biol.* 2010;55:483-495.

12. Liu H, Ren G, Miao Z, et al. Molecular optical imaging with radioactive probes. *PLoS One.* 2010;5:e9470.

13. Warburg O. On the origin of cancer cells. *Science.* 1956;123:309-314.

14. Lin H, Zhang R, Gunn JR, et al. Comparison of Cherenkov excited fluorescence and phosphorescence molecular sensing from tissue with external beam irradiation. *Phys Med Biol.* 2016;61:3955-3968.

15. *Guide for the Care and Use of Laboratory Animals*. Washington, DC: National Academy Press; 1996.

16. Lee KH, Ko BH, Paik JY, et al. Effects of anesthetic agents and fasting duration on 18F-FDG biodistribution and insulin levels in tumor-bearing mice. *J Nucl Med.* 2005;46:1531-1536.

17. Sinha RP, Hader DP. UV-induced DNA damage and repair: a review. *Photochem Photobiol Sci.* 2002;1:225-236.

18. Rastogi RP, Richa, Kumar A, Tyagi MB, Sinha RP. Molecular mechanisms of ultraviolet radiation-induced DNA damage and repair. *J Nucleic Acids.* 2010;2010:592980.

19. Malaise EP, Fertil B, Chavaudra N, Guichard M. Distribution of radiation sensitivities for human tumor cells of specific histological types: comparison of in vitro to in vivo data. *Int J Radiat Oncol Biol Phys.* 1986;12:617-624.

20. Pauwels EK, Sturm EJ, Bombardieri E, Cleton FJ, Stokkel MP. Positron-emission tomography with [18F]fluorodeoxyglucose. Part I. Biochemical uptake mechanism and its implication for clinical studies. *J Cancer Res Clin Oncol.* 2000;126:549-559.

21. Ruggiero A, Holland JP, Lewis JS, Grimm J. Cerenkov luminescence imaging of medical isotopes. *J Nucl Med.* 2010;51:1123-1130.

22. Beattie BJ, Thorek DL, Schmidtlein CR, Pentlow KS, Humm JL, Hielscher AH. Quantitative modeling of Cerenkov light production efficiency from medical radionuclides. *PLoS One.* 2012;7:e31402.

23. Kotagiri N, Sudlow GP, Akers WJ, Achilefu S. Breaking the depth dependency of phototherapy with Cerenkov radiation and low-radiance-responsive nanophotosensitizers. *Nat Nanotechnol.* 2015;10:370-379.

24. Kamkaew A, Cheng L, Goel S, et al. Cerenkov radiation induced photodynamic therapy using chlorin e6-loaded hollow mesoporous silica nanoparticles. *ACS Appl Mater Interfaces.* 2016;8:26630-26637.

25. Sato K, Sato N, Xu B, et al. Spatially selective depletion of tumor-associated regulatory T cells with near-infrared photoimmunotherapy. *Sci Transl Med.* 2016;8:352ra110.

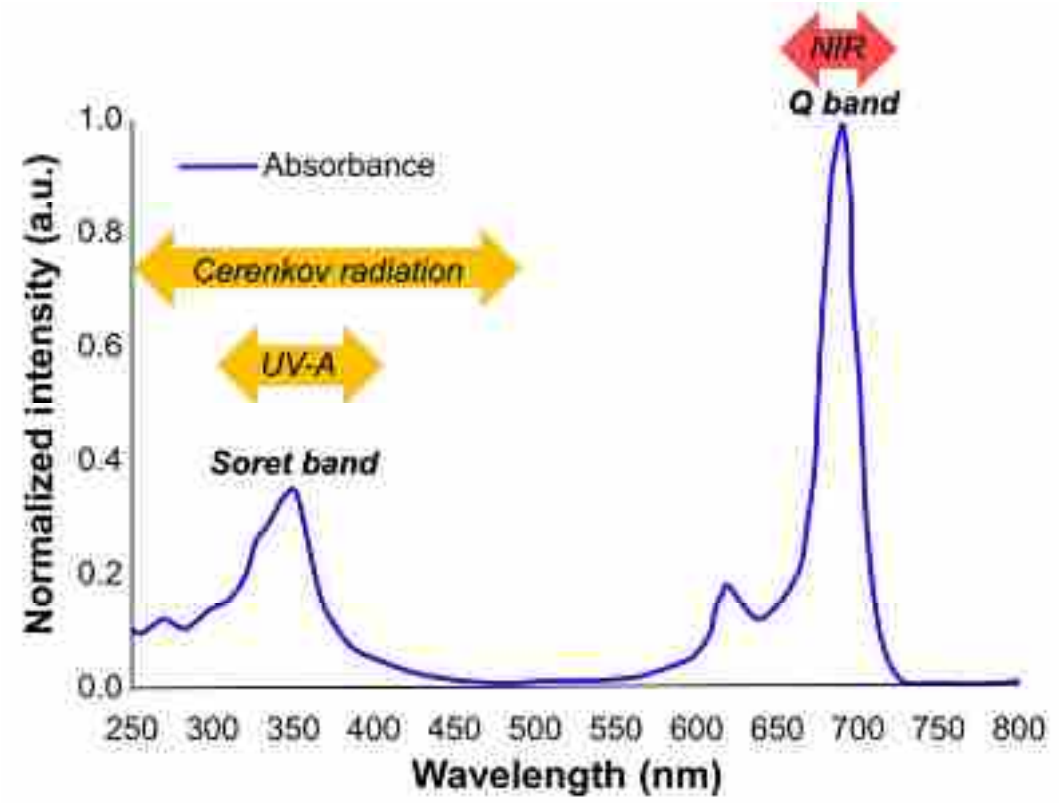

Fig. 1

Absorption spectra of IRDye 700DX.

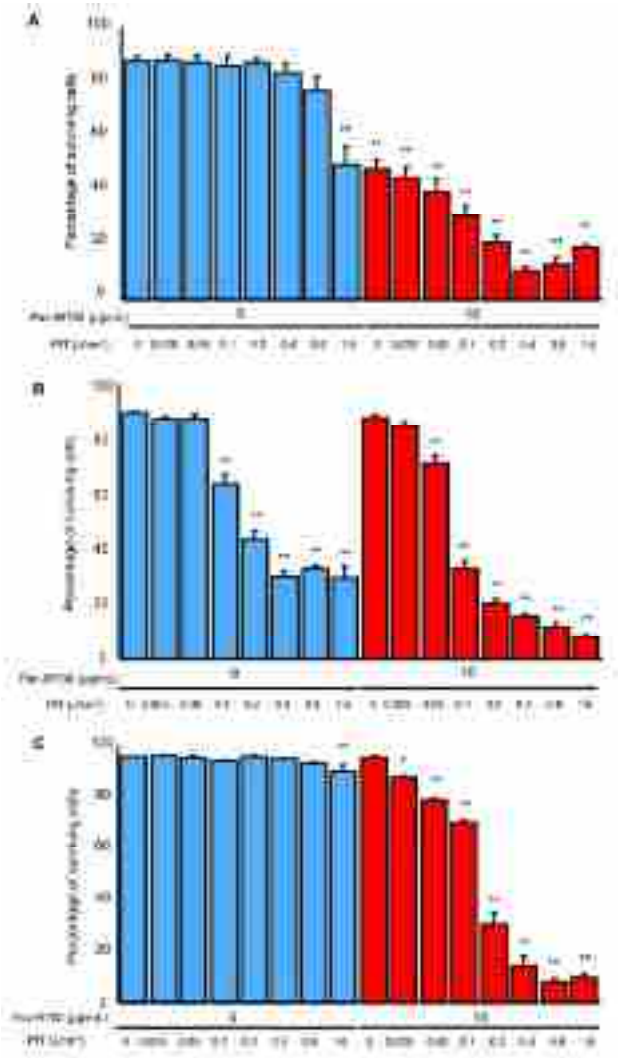

Fig. 2

Evaluation of *in vitro* UV-A-PIT (*p<0.05, **p < 0.01, vs untreated control). (A) Percentage of surviving cells decreased in a light dose dependent manner although 50 % of A431 cells died when pan-IR700 alone without UV-A light was administered. (B) propidium iodide staining showed membrane damage in

MDAMB468-luc cells induced by UV-A-PIT although significant cytotoxicity associated with UV-A light alone was observed. (C) With tra-IR700 the percentage of surviving 3T3/HER2-luc cells decreased in a light dose dependent manner

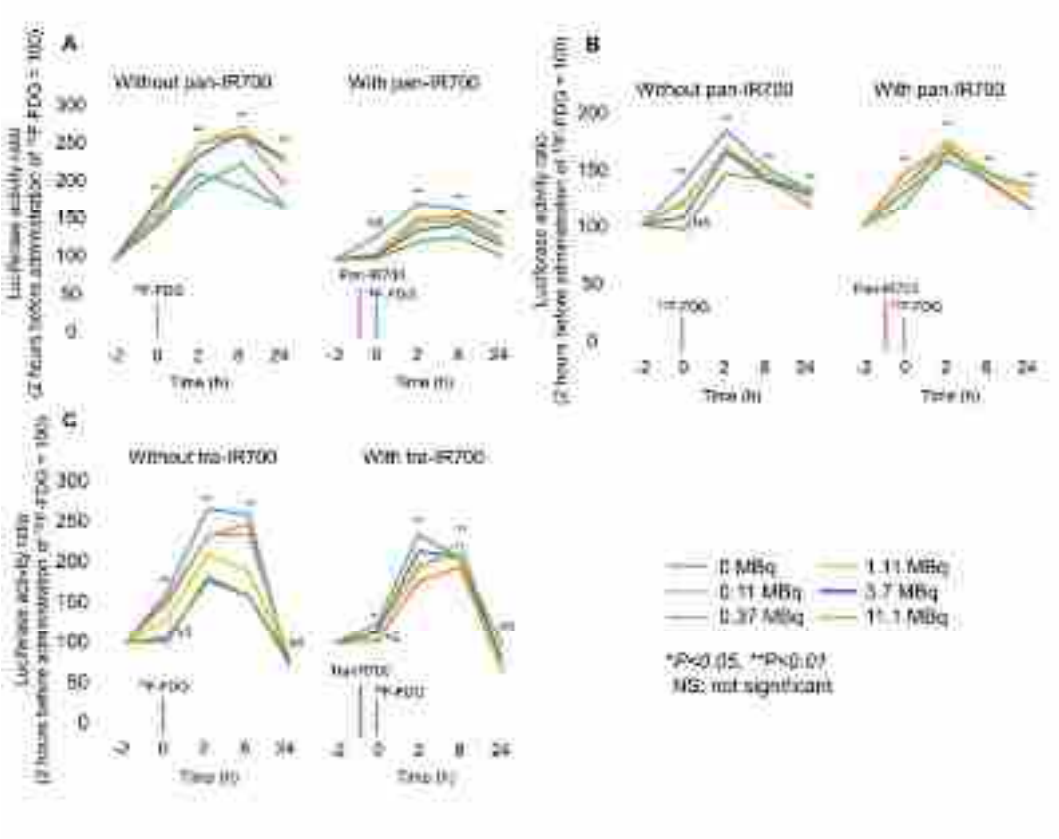

Fig. 3

Evaluation of *in vitro* CR-PIT using ^{18}F-FDG. (A) Using A431-luc cells suppression of luciferase activity in cells was seen in CR-PIT and the degree of suppression increased in a dose dependent manner. (B) Using MDAMB468-luc cells CR-PIT did not significantly change the level of luciferase activity compared to ^{18}F-FDG alone. (C) Using 3T3/HER2-luc cells CR-PIT also did not significantly change the level of luciferase activity compared to ^{18}F-FDG alone.

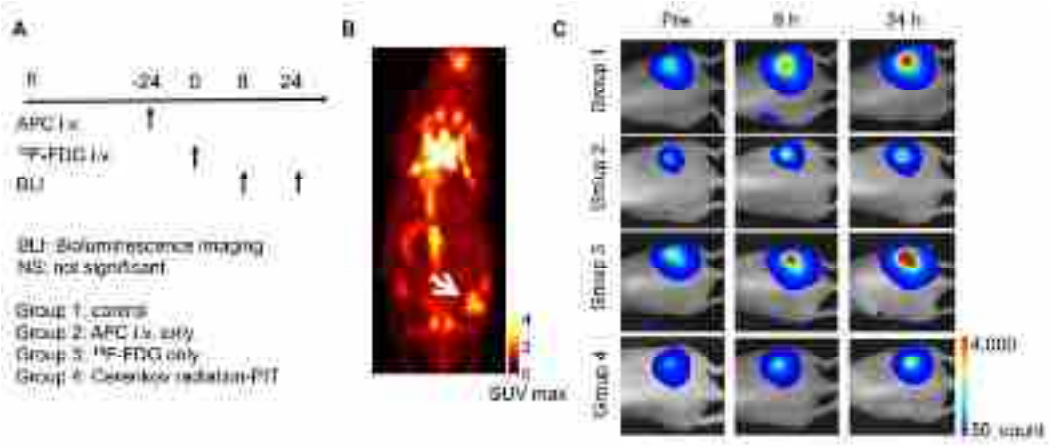

Fig. 4

In vivo effect of CR-PIT on A431-luc tumor. (A) CR-PIT regimen is shown. (B) ^{18}F-FDG PET imaging of tumor bearing mice. Tumor showed high accumulation of ^{18}F-FDG (arrow). (C) Bioluminescence imaging of tumor-bearing mice.

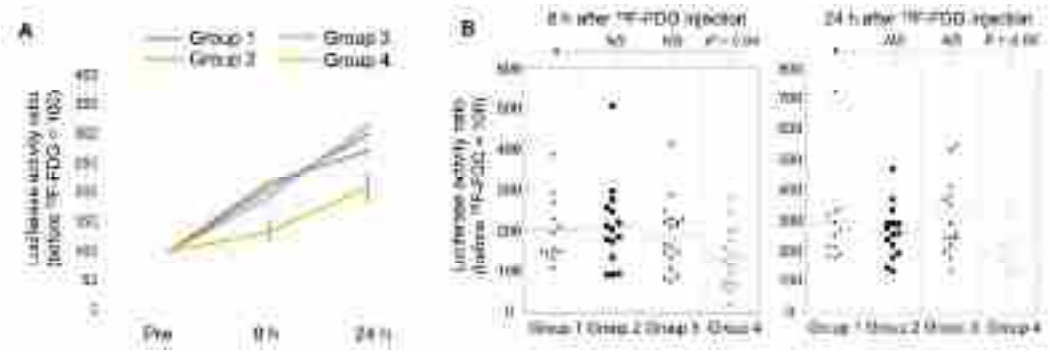

Fig. 5

In vivo effect of CR-PIT on A431-luc tumor. (A) Luciferase activity ratio was suppressed in CR-PIT group compared to the control group. (B) Significant suppression of luciferase activity ratio was seen in CR-PIT group compared to control group.

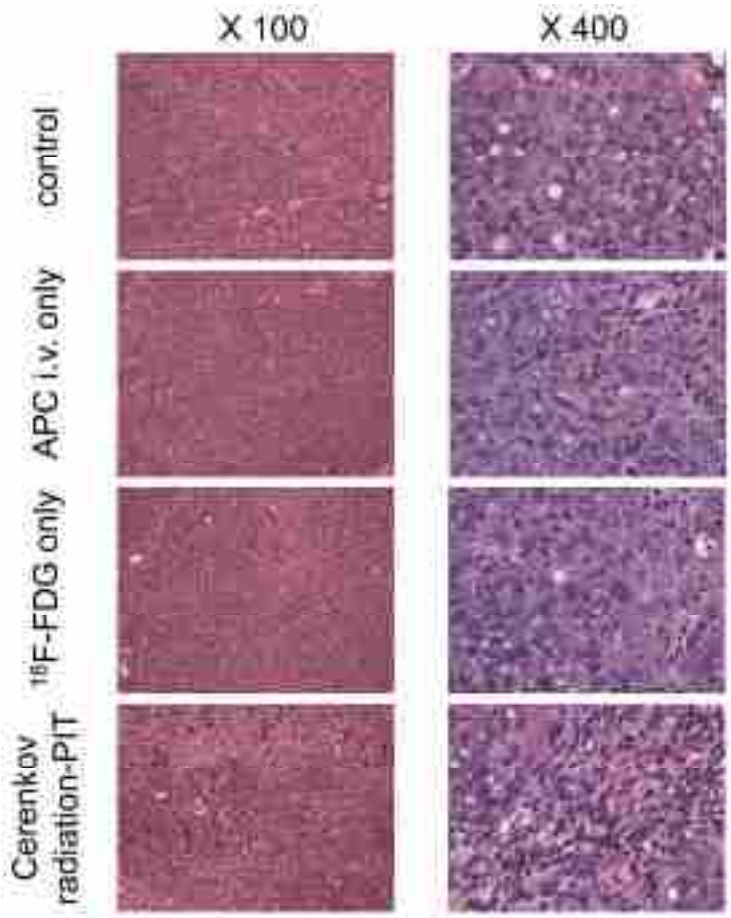

Fig. 6

Resected tumors stained with hematoxylin and eosin. Cellular necrosis and micro-hemorrhage were seen within a background of live but damaged tumor cells after CR-PIT while little damage was observed in tumors receiving ^{18}F-FDG administration alone. No obvious damage was observed in the tumor receiving only APC but no ^{18}F-FDG administration.

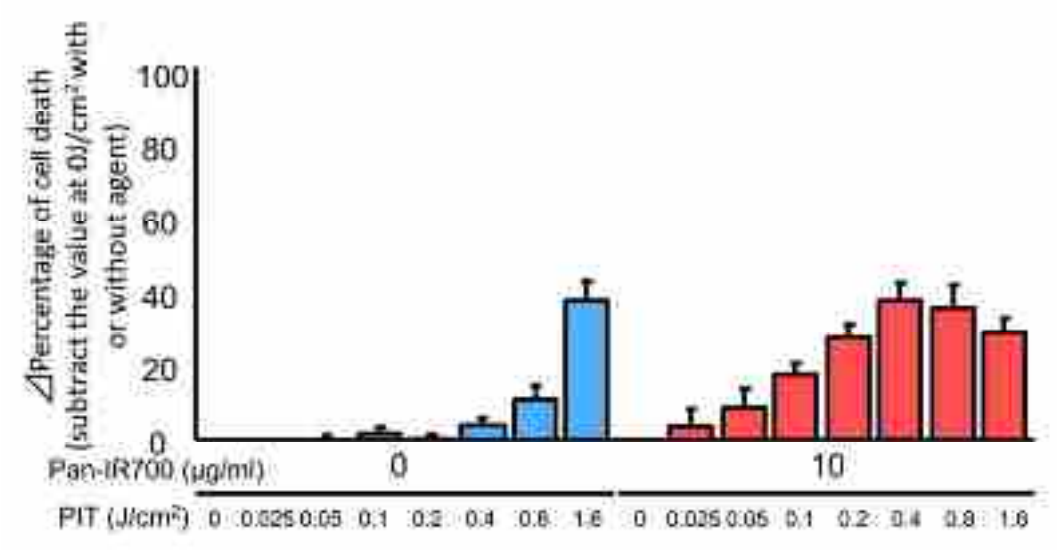

Supplemental Fig. 1

Δ percentage of surviving cells, the difference between the value without UV-A light with or without pan-IR700, increased in a light dose dependent manner with pan-IR700.

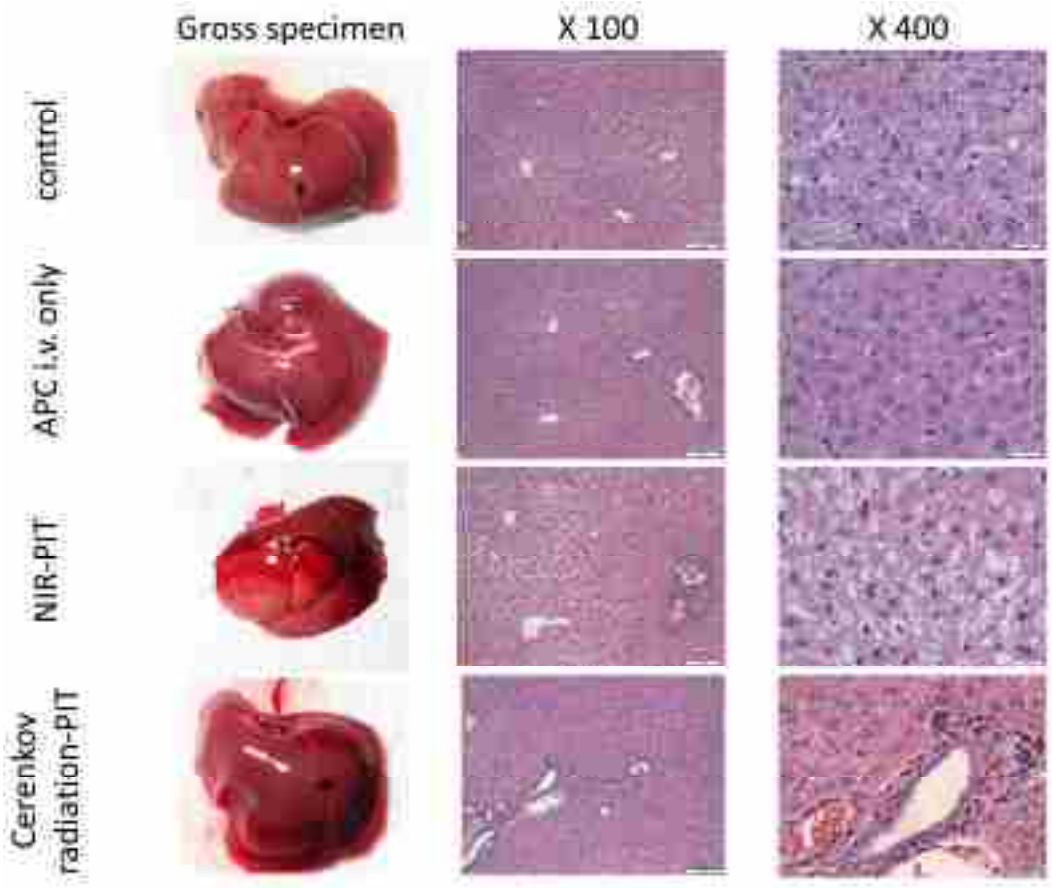

Supplemental Fig. 2

Gross specimen and microscopic images stained with hematoxylin and eosin of extracted livers. In liver treated with NIR-PIT color in the irradiated area was changed in white macroscopically. In addition, obvious hepatic cell damage was confirmed microscopically. On the other hand, in liver treated with CR-PIT mild hepatic cell damage was confirmed in peri-Glisson's capsule area although there

was no obvious change in gross appearance. No obvious damage was observed in livers in the APC i.v. only and control groups.

The Journal of NUCLEAR MEDICINE

Cerenkov radiation-induced photoimmunotherapy with ^{18}F-FDG

Yuko Nakamura, Tadanobu Nagaya, Kazuhide Sato, Shuhei Okuyama, Fusa Ogata, Karen J Wong, Stephen Adler, Peter L Choyke and Hisataka Kobayashi

J Nucl Med.
Published online: April 13, 2017.
Doi: 10.2967/jnumed.116.188789

The Journal of Nuclear Medicine is published monthly.
SNMMI | Society of Nuclear Medicine and Molecular Imaging
1850 Samuel Morse Drive, Reston, VA 20190.
(Print ISSN: 0161-5505, Online ISSN: 2159-662X)

SNMMI SOCIETY OF NUCLEAR MEDICINE AND MOLECULAR IMAGING